JOURNAL OF COMPUTATIONAL PHYSICS 47, 352–374 (1982)

High Level Continuity for Coordinate Generation with Precise Controls

PETER R. EISEMAN*

Department of Applied Physics and Nuclear Engineering, Columbia University, New York, New York 10027

Received November 20, 1981

The development of precisely controlled coordinate generation techniques is continued from a first study to include the higher order smoothness which is necessary for three-dimensional applications. In the first study, the controls came from the use of local piecewise linear interpolants in the general multisurface transformation. The consequent integration therein resulted in coordinates with continuity up to first derivatives and with the capability to prescribe uniformity either locally or globally for the family of transverse coordinate curves. The admission of uniformity placed a constraint upon the general interpolants which was trivially satisfied in the piecewise linear case. With smoother piecewise constructions, the constraint is used herein along with a requirement for coordinate curves to have the most general possible curvature properties. The result is a class of coordinate transformations with continuity extended up to higher derivatives that retains the precise local controls displayed in the first study and that can be used in three or more dimensions.

INTRODUCTION

The present study is a continuation in the development of precise controls for coordinate generation. Precise controls were established in the first study [1] when local piecewise linear interpolants ψ_k were employed within the context of the general multisurface transformation. With N surfaces, an interpolant is assigned to each point r_k of a partition $r_1 < r_2 < \cdots < r_{N-1}$ for the independent variable r that is transverse to the surfaces. Each partition point corresponds to a space between the N surfaces $\mathbf{P}_1(\mathbf{t}), \mathbf{P}_2(\mathbf{t}),..., \mathbf{P}_N(\mathbf{t})$ that are ordered from bounding surface to bounding surface and that are parameterized by a common surface coordinate vector $\mathbf{t}$. For general interpolants ψ_k, the multisurface transformation $\mathbf{P}(r, \mathbf{t})$ is given by

$$\mathbf{P}(r, \mathbf{t}) = \mathbf{P}_1(\mathbf{t}) + \sum_{k=1}^{N-1} \frac{G_k(r)}{G_k(r_{N-1})} [\mathbf{P}_{k+1}(\mathbf{t}) - \mathbf{P}_k(\mathbf{t})], \tag{1a}$$

* Research performed under AFOSR Contract No. F49620-79-C-0132. Partial support was supplied under NASA Contract No. NAS1-15810 while the author was in residence at the Institute for Computer Applications in Science and Engineering, NASA Langley Research Center, Hampton, Va. 23665.

0021-9991/82/090352-23$02.00/0

where

$$G_k(r) = \int_{r_1}^{r} \psi_k(x)\, dx \tag{1b}$$

and each $\psi_k(r_i)$ vanishes unless $k = i$. In the first study, an admissibility condition for r-direction uniformity was established as a constraint on the general interpolants ψ_k which is given by

$$\sum_{k=1}^{N-1} \frac{\psi_k(r)}{\psi_k(r_k)} = 1. \tag{2}$$

Inadmissible interpolants could not be used to prescribe a uniform distribution of the constant r coordinate surfaces even on a local basis. Such prescriptions formed the foundation from which mesh structures could be specified over regional volumes. With the local piecewise linear interpolants that were examined there in detail, the admissibility of uniformity was trivially satisfied. The interpolants were nonvanishing on the smallest possible interval defined by the partition points r_k and belonged to the class C^0 of continuous functions. From the multisurface integration of Eq. (1b), the coordinates belonged to the continuity class C^1 of continuous (vector) functions with continuous first derivatives. The C^1 coordinates are, however, generally applicable only for two-dimensional systems. In three dimensions, only special cases such as rotationally symmetric systems can be considered.

When a numerical solution is contemplated for a boundary value problem with a fully three-dimensional configuration or with a need for second derivatives of geometric quantities, the local C^0 interpolates that were examined previously [1] must be replaced by local C^1 interpolates. The local C^1 interpolates clearly lead to C^2 coordinates due to the substitution into the integrands of the multisurface transformation. With a C^2 transformation, each coordinate curve is continuously differentiable up to second order; hence, the coordinate curve curvature can be continuous (cf. [2]). In addition, for points with nonvanishing curvature, the Frenet frame attached to the curve can also be continuously defined; the implication is that a coordinate curve can continuously bend out of a plane, as opposed to being constrained to a plane or leaving a plane only with vanishing curvature. For the out-of-plane bending to be differentiable, another derivative of the coordinate transformation would be needed in order to define the torsion of the coordinate curves. On segments with vanishing torsion, a curve is constrained to a plane; otherwise, it is bending out of the plane. In view of the fact that coordinate curves in three dimensions generally would not be constrained to planes (even locally), the minimum requirement for coordinate generation in three dimensions would be that the bending process is continuous; hence, the coordinate transformation must at least be of class C^2. In the present study, the transformations are developed for continuity levels of C^2 and higher. The emphasis is placed on C^2, which yields the simplest generally applicable methods for three dimensions and which has controls that are more local than for the

higher levels. At each level, the size of each region (between partition points of r) and the shape of each interpolation function is chosen so that certain important properties such as uniformity in r are admissible. In the C^2 case, the curvature of coordinate curves in r is a property that is not to depend overly on the C^1 interpolants. The assumption here is that flat spots are not to appear arbitrarily from the construction process. Under the general constraint of simplicity, the C^2 coordinates are developed in detail and the subsequent forms for higher continuity levels are taken as continuations from the established pattern.

The Form of the C^1 Interpolates

Although it is possible to arbitrarily construct interpolation functions which vanish outside of local intervals determined by the partition points and which are continuous up through first derivatives, the family of interpolation functions derived from such an unconstrained construction will in general *not* lead to a system of multisurface coordinates where uniformity in the distribution of constant r surfaces can be specified or where unspecified flat spots (vanishing curvature) can be prevented along coordinate curves in the r variable. To construct only those coordinate systems where uniformity can be specified and where flat spots do not arbitrarily appear, the family of interpolation functions must be suitably constrained. To further require that the local intervals are as small as possible will result in a basic family of interpolates. Since an interpolate for the multisurface transformation must vanish at all partition points except one, the smallest possible interval would be determined by at least three successive partition points. The reason is that the nonvanishing at a partition point will extend by continuity to either side of the point. This extension by continuity is meaningful only when the point is not one of the endpoints r_1 or r_{N-1}. Since the interpolates at endpoints are essentially truncated versions of an interior interpolate, the discussion will focus only on interpolants at interior points.

Suppose now that the smallest possible interval associated with any interior partition point r_k is precisely the interval from r_{k-1} to r_{k+1}. A schematic illustration of the interpolation function ψ_k is then given in Fig. 1. Since ψ_k vanishes outside of the interval $[r_{k-1}, r_{k+1}]$ and is a continuous function with continuous first derivatives, its function values and first derivatives must vanish at r_{k-1} and r_{k+1}. The

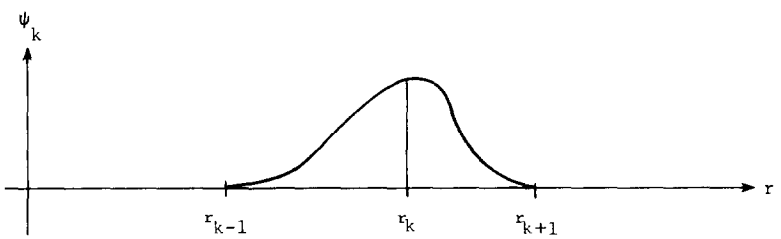

FIG. 1. A C^1 interpolation function over three partition points.

only other interpolation functions which do not vanish on the interval $[r_{k-1}, r_{k+1}]$ are interpolation functions ψ_{k-1} and ψ_{k+1} that are respectively centered about the endpoints of the interval. By the same reasoning, both function values and first derivatives of ψ_{k-1} and ψ_{k+1} must vanish at r_k. Consequently, the only possibility for the entire interpolation to have a nonzero first derivative at r_k is for ψ_k to have a nonzero first derivative at r_k. In terms of the multisurface transformation, the variable r coordinate curves have a nonzero second derivative at r_k only if the first derivative of ψ_k is nonzero at r_k. Since the curvature of the coordinate curves is directly proportional to the normal component of the second derivative, only a nonzero first derivative of ψ_k at r_k can prevent the appearance of a flat spot (vanishing curvature) at r_k. Now, to obtain a uniform distribution of the constant r coordinate surfaces, the variable r coordinate curves must first be projected along a sufficiently smooth vector field which can be used as a reasonable measure for the desired uniformity. Uniformity is then achieved when the variable r is a linear function of the arc length along the vector directions. For uniformity to be possible, the condition upon the interpolation functions is given by Eq. (2). To specify local uniformity in a neighborhood of r_k, the condition must be satisfied there, and in particular, the derivative of Eq. (2) must also be satisfied at r_k. Since $\psi_k(r_k) \neq 0$, however, the derivative $\psi_k'(r_k)$ must then vanish, which in turn contradicts the desire not to have a flat spot arbitrarily appear at r_k. Consequently, to admit the possibility of uniformity and to avoid any unspecified flat spots, the size of the interval in the r variable must be increased to extend beyond a sequence of three partition points. By symmetry, the interval for r must be determined by at least five successive partition points with shorter intervals only near the boundaries r_1 and r_{N-1} due to an obvious truncation for each of the two closest interpolation functions to each boundary. For reference, the above discussion is summarized in the following theorem:

THEOREM 1. *Let $r_1 < r_2 < \cdots < r_{N-1}$ be a partition for the multisurface transformation and let $\mathscr{C}$ be the class of all real valued functions which are defined on the interval $r_1 \leqslant r \leqslant r_{N-1}$ and which satisfy the following properties*:

(1) *The functions and their first derivatives are continuous*;

(2) *Each function is nonzero on only one partition point*;[1]

(3) *Unspecified flat spots do not appear along the coordinate curves in variable r*;

(4) *A uniform distribution of the constant r coordinate surfaces can be specified either locally or globally*; *and*,

(5) *The intervals on which each function does not vanish are as small as possible.*

For any function f in $\mathscr{C}$, let $D(f)$ be the domain $\{r \mid f(r) \neq 0\}$ of nonvanishing values.

[1] This condition is the cardinality property required by the multisurface transformation. It is needed; otherwise, the normalization process in the multisurface transformation would be lost.

Then, among the intervals determined by partition points, the smallest interval containing $D(f)$ must be selected from:

$$[r_1, r_3], [r_1, r_4], [r_1, r_5], \ldots, [r_{k-2}, r_{k+2}], \ldots, [r_{N-5}, r_{N-1}], [r_{N-4}, r_{N-1}], [r_{N-3}, r_{N-1}]$$

or a larger interval which strictly contains one of these listed intervals.

In three dimensions, the minimum interval size derived above is particularly evident on purely geometric grounds. To see why, suppose that the smaller interval lengths are used, and consider values of r between r_k and r_{k+1} for some fixed k. Then the vector field interpolation consists of only contributions from ψ_k and ψ_{k+1}; consequently, the multisurface transformation reduces to a linear combination of the vectors $\mathbf{P}_k$, $(\mathbf{P}_{k+1} - \mathbf{P}_k)$, and $(\mathbf{P}_{k+2} - \mathbf{P}_{k+1})$ which can be rewritten as a linear combination of $\mathbf{P}_k$, $\mathbf{P}_{k+1}$, and $\mathbf{P}_{k+2}$. The implication here is that for $r_k \leqslant r \leqslant r_{k+1}$, the coordinate curve in the variable r lies in the plane determined by these three points. For an adjoining interval, a similar arguement implies that there is a similar three point dependence. For example, with $k > 1$ the curve depends only on $\mathbf{P}_{k-1}$, $\mathbf{P}_k$, and $\mathbf{P}_{k+1}$ when $r_{k-1} \leqslant r \leqslant r_k$. Now if the vectors $\mathbf{P}_{k-1}$, $\mathbf{P}_k$, $\mathbf{P}_{k+1}$, and $\mathbf{P}_{k+2}$ are not coplanar, then the planar restrictions on either side of r_k would imply that the unit normal and binormal vectors are discontinuous at r_k. Also at r_k, the coordinate curve passes through the intersection of the planes, and moreover, by direct calculation, both first and second r-derivatives of the transformation are proportional to $\mathbf{P}_{k+1} - \mathbf{P}_k$ and are continuous. Since the second arc length derivative is proportional to a linear combination of the first and second r-derivatives, and in addition, is equal to the product of curvature with the unit normal vector, the curvature must vanish because of the orthogonallity between tangent and normal vectors. Here, the discontinuous unit normal vector at r_k can be taken as the limiting value from either side of r_k. An illustration of the problem is given by the example in Fig. 2.

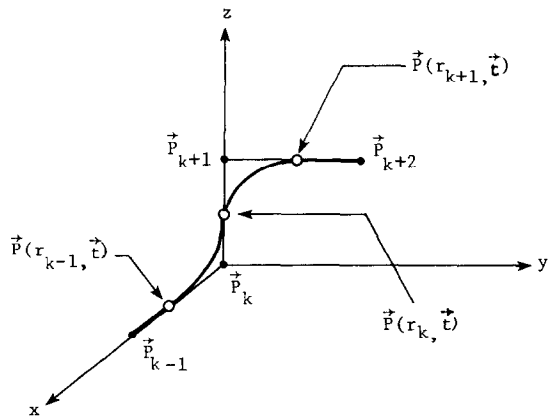

FIG. 2. Example of a three-dimensional coordinate curve with local basis functions which vanish off intervals determined by only three successive partition points.

In the figure, a coordinate curve in the variable r is given where, $\mathbf{P}_k$ is the origin, $\mathbf{P}_{k-1}$ is on the positive x axis, $\mathbf{P}_{k+1}$ is on the positive z axis, and $\mathbf{P}_{k+2}$ is in the $y-z$ plane along a line from $\mathbf{P}_{k+1}$ which is parallel to the y axis. As r goes from r_{k-1} to r_k the curve leaves the x axis, remains in the $x-z$ plane, and approaches the z axis where it has a tangent vector in the positive z direction. As r goes from r_k to r_{k+1}, the curve leaves the z axis with the same tangent in the positive z direction, remains entirely in the $y-z$ plane, and approaches the line from $\mathbf{P}_{k+1}$ which is parallel to the y axis. The unit normal vectors are contained in the $x-z$ plane for $r < r_k$ and in the $y-z$ plane for $r > r_k$. The result is a 90 degree rotation of the normal vector about the tangent direction (z axis) at r_k. A similar rotation is also observed for the unit binormal vectors which are constants respectively parallel to the y and x axes. Since the arc length derivative of the unit binormal vector vanishes on either side of r_k, the torsion of the curve, from its definition, also vanishes. At r_k, the torsion is clearly undefined. Analytically, three derivatives would be needed. With the exception of the analytically observed vanishing of curvature at r_k, the example illustrates the constraints placed upon the interpolation functions when three-dimensional applications are considered. For three-dimensional applications, Theorem 1 can then be restated as follows:

THEOREM 2. *If the requirement for uniformity in Theorem* 1(4) *is replaced by a requirement for applicability to three dimensions, then the conclusion of Theorem* 1 *is again true.*

From the conclusion above, that the interpolation functions must nontrivially extend over intervals which can be no smaller than a certain size, there is no condition on the complexity of the functions. Without any assumptions, they can have any arbitrarily large number of local extrema whether or not they are constrained to the smallest permissible intervals. For simplicity, the candidate interpolation functions will now be assumed to have a minimal number of extrema, to be constrained to the smallest intervals which may be permissible, and to have maximum values at points of interpolation. In geometric terms, the latter condition may be thought of as a requirement that each function be well centered about the partition point associated with its interpolatory contribution. In Fig. 3, the form of the candidate interpolation functions are illustrated for each partition point. The most complete function is the interpolation function ψ_k corresponding to the partition point r_k for $2 < k < N-2$. From the illustration in Fig. 3c, this interior function ψ_k is easily seen to have three extrema: a maximum at r_k, a minimum to the left of r_{k-1}, and a minimum to the right of r_{k+1}. Since ψ_k must vanish at partition points unequal to r_k, the minimum values must either be negative or zero. A minimum value of zero, however, is not permitted. Otherwise, there would be more extrema than desired or else the function would be nontrivial on too small of an interval. Since ψ_k has continuous first derivatives and vanishes outside of the interval $[r_{k-2}, r_{k+2}]$, there is an inflection point between each minimum and its join with a part of the r axis. The inflection occurs because the derivative of ψ_k is a continuous function which

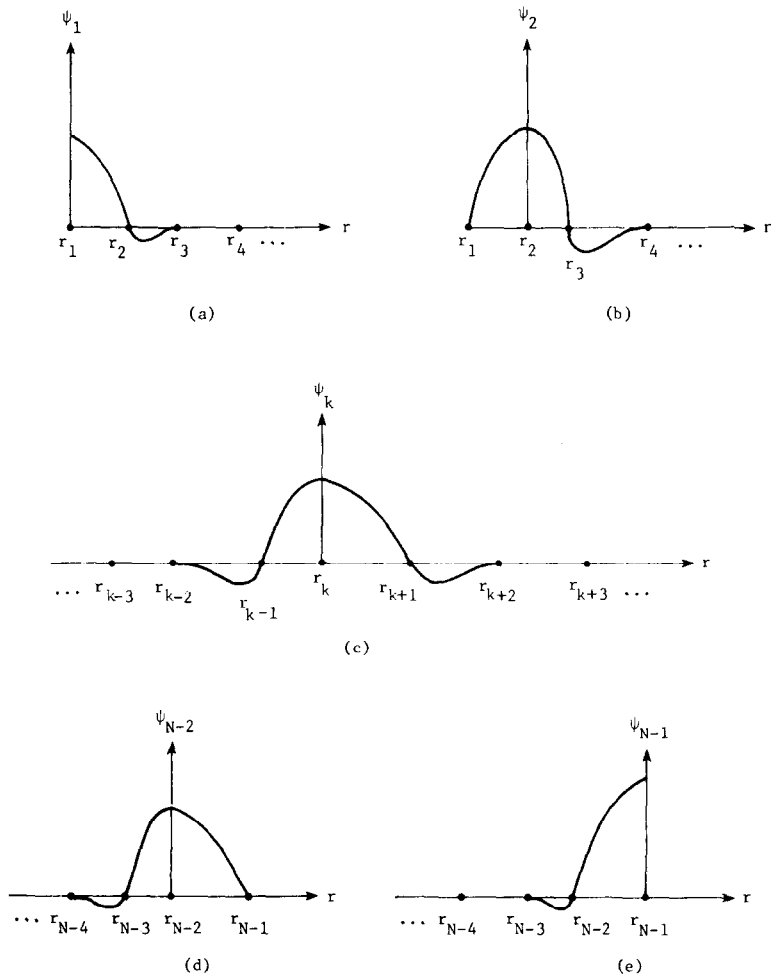

FIG. 3. Schematic form of the simplest C^1 interpolation functions for the partition $r_1 < r_2 < \cdots < r_{N-1}$.

monotonically approaches a single extremum value from zero values at the outer endpoints of the two respective intervals. Consequently, on each interval, the ψ_k tangent line at the extremum cuts the locus of points determined by ψ_k into segments on opposite sides of the line; hence, by definition, there is an inflection point. By similar reasoning, there is also a single inflection point between each minimum of ψ_k and r_k. In total, the function ψ_k has precisely four inflection points. The form of the most complete interpolation function ψ_k also carries over, in part, to the functions associated with each boundary point and its closest partition point. With the closest partition points, the interpolation functions are simply truncated versions of the

complete function obtained by the removal of one of the endpoint intervals. In Figs. 3b and d, the functions ψ_2 and ψ_{N-2}, associated with r_2 and r_{N-2} are illustrations: the truncation is obtained with the removal of $[r_{k-2}, r_{k-1})$ or $(r_{k+1}, r_{k+2}]$, respectively. In a similar manner, the endpoint interpolation functions ψ_1 and ψ_{N-1} are also truncated. Clearly, $[r_{k-2}, r_k)$ or $(r_k, r_{k+2}]$ must be removed. Since the maximum value does not have to be a local maximum, however, the slope of ψ_1 at r_1 or ψ_{N-1} at r_{N-1} need not be zero. An illustration of these respective functional forms appears in Figs. 3a and e.

With the simple functional forms given in Fig. 3, the question remains as to whether or not these forms will yield coordinate transformations where uniformity in the distribution of constant r surfaces can be specified and where unspecified flat spots can be avoided. An application to three dimensions, however, is not a problem since a coordinate curve in the variable r can bend out of a plane in a continuous manner with a continuous (although not differentiable) Frenet frame. To obtain functional forms which are computationally efficient, a piecewise polynomial representation of minimal degree will be considered and will lead to an affirmative answer to the remaining question above. Since piecewise linear functions cannot yield the desired functional forms with continuous derivatives, piecewise quadratics must be considered. To further simplify the representation, a minimal number of polynomial segments will be assumed. With the quadratics, the minimum number will be obtained with precisely two segments between every pair of partition points so that the inflection points in the functional forms can be modeled. To ensure that interpolation functions corresponding to distinct interpolation points can be added without an increase in the number of polynomial segments on any interval (r_k, r_{k+1}), a single juncture point will be assumed for each interval, independent of any particular interpolation function. For each interval (r_k, r_{k+1}), the piecewise quadratics for each interpolation function will now have a single juncture at a point $w_k = r_k + \alpha_k h_k$, where $h_k = r_{k+1} - r_k$ and α_k is a fixed real number between 0 and 1. Without any constraints, the general piecewise quadratic representations just described will not yield the desired uniformity and nonflatness properties. However, since the piecewise polynomials have juncture points which are aligned at partition points r_k and at the internal points $w_k = r_k + \alpha_k h_k$, conditions for uniformity and nonflatness can be applied at such points. The result will be the class of all piecewise quadratics with the desired properties. Moreover, the existence of this class of functions will remove any requirement for the interpolation functions to be nontrivially defined over larger intervals. Consequently, the possibility of the larger intervals can be deleted from Theorem 1.

Piecewise Quadratic Interpolation Functions

The piecewise quadratic representation described in the previous section will now be explicitly derived. Although a direct derivation would be possible, an easier and clearer method is to derive first the derivative functions and then obtain the inter-

polation functions by integration. Since the piecewise quadratic functions have continuous first derivatives, the derivative functions are clearly continuous piecewise linear functions, and consequently, have the advantage of being completely specified by their function values at junctures between their linear segments. In Fig. 4, the piecewise linear derivative functions are illustrated in an order that corresponds with the functional forms of Fig. 3. With the exception of the boundary functions ψ_1 and ψ_{N-1}, the derivative evaluations $\psi_k'(r_k)$ must vanish so that each interpolation

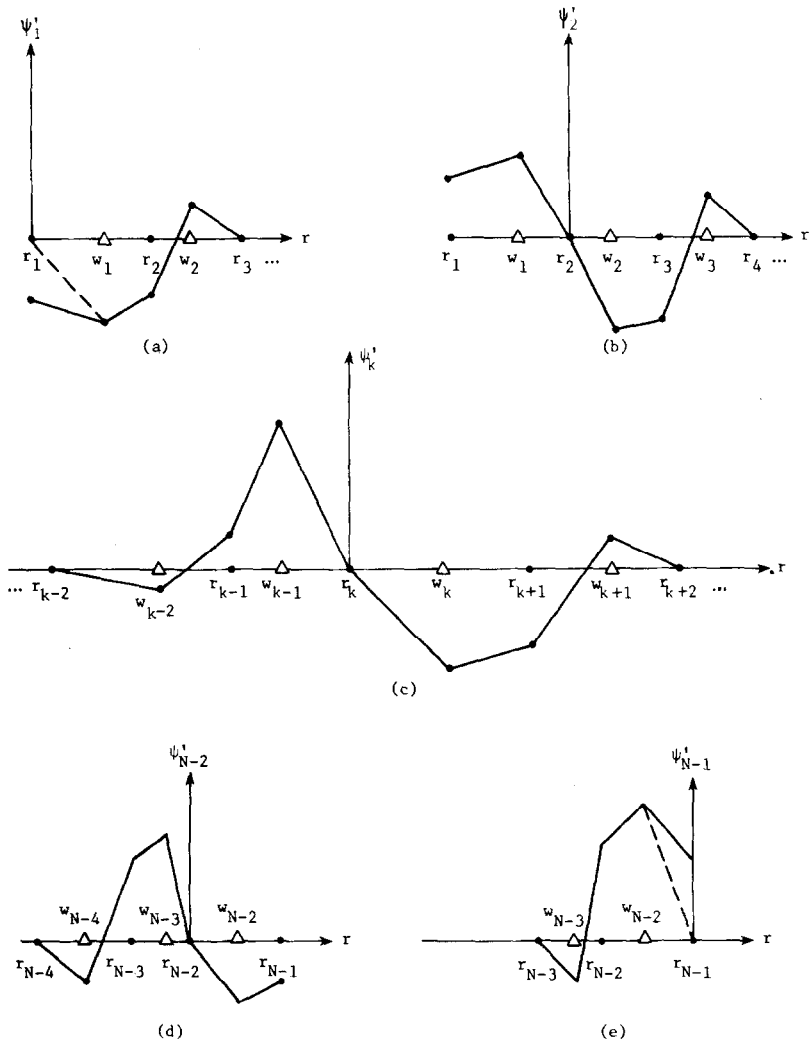

FIG. 4. Derivatives of the piecewise quadratic interpolation functions defined from the interlaced mesh $r_1 < w_1 < r_2 < \cdots < w_{N-2} < r_{N-1}$ and in correspondence with the functional forms illustrated in Fig. 3. Partition points r_k ($\cdot$) and intermediate juncture locations w_k ($\triangle$).

function ψ_k is centered about a local maximum at its corresponding partition point r_k, as illustrated in Figs. 3b–d and 4b–d. The maximum values for the boundary functions, however, need not be local maximums in the sense of vanishing derivatives. These nonvanishing derivatives are illustrated by the replacement of the dashed line by the solid line in Figs. 4a and e. Since ψ_k must vanish at partition points unequal to r_k, the derivative function ψ_k' must integrate to zero over the intervals $[r_{k-2}, r_{k-1}]$ and $[r_{k+1}, r_{k+2}]$ whenever they are defined. The consequence is a relationship between the nontrivial function values of ψ_k' at mesh points on these intervals. The relationship is expressed in the following lemma:

LEMMA 1. *Let ψ_k be the piecewise quadratic interpolation functions defined on the interlaced mesh $r_1 < w_1 < r_2 < \cdots < r_{N-2} < w_{N-2} < r_{N-1}$, where $w_k = r_k + \alpha_k h_k$ with $h_k = r_{k+1} - r_k$ and $0 < \alpha_k < 1$ for $k = 1, 2, \ldots, N-2$. Then the derivative functions ψ_k', centered at r_k, satisfy the left of center relationships*

$$\psi_k'(w_{k-2}) = -(1 - \alpha_{k-2})\, \psi_k'(r_{k-1}), \tag{3a}$$

for $k = 3, 4, \ldots, N-1$; and the right of center relationships

$$\psi_k'(w_{k+1}) = -\alpha_{k+1}\, \psi_k'(r_{k+1}), \tag{3b}$$

for $k = 1, 2, \ldots, N-3$.

Proof. From an examination of the derivative functions ψ_k' which are illustrated in Fig. 4, the functional forms to the right of center are observed to be reflections of those on the left: the reflections are about the form centers and about the r axis. In particular, the right of center relationship is just the reflected image of a left of center relationship. Consequently, it is sufficient to consider only the left of center case which is illustrated in Fig. 5. For simplicity, the notation $a = -\psi_{m+2}'(r_m + \alpha_m h_m) > 0$

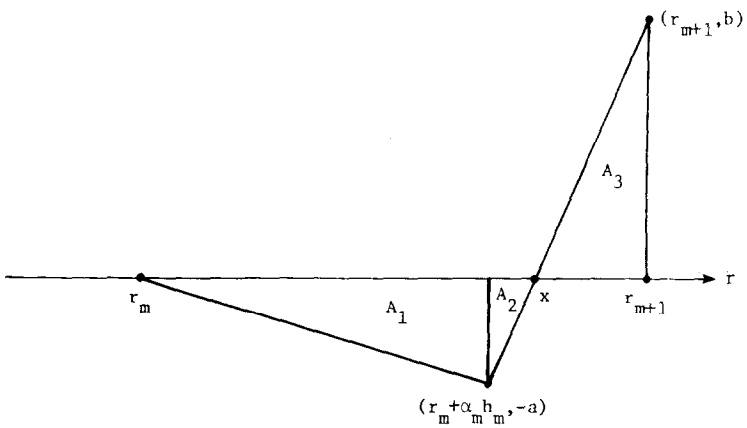

FIG. 5. A part of a derivative function on the left.

and $b = \psi'_{m+2}(r_{m+1}) > 0$ is used. In terms of this notation and the point x where ψ'_{m+2} crosses the r-axis, the areas of the right hand triangles in the figure are given by $A_1 =$ [illegible] obtained from the linear equation

$$\psi'_{m+2}(x) = [(a+b)/(1-\alpha_m)\,h_m][x - r_m - \alpha_m h_m] - a = 0. \tag{4}$$

By substitution for x, the last two areas now become $A_2 = a^2(1-\alpha_m)\,h_m/2(a+b)$ and $A_3 = b^2(1-\alpha_m)\,h_m/2(a+b)$. Since $\psi_{m+2}(r_{m+1}) = 0$, the area $A_1 + A_2$ below the r-axis must be equal to the area A_3 above it. Upon simplification, the equation $A_1 + A_2 = A_3$ then reduces to $a = (1-\alpha_m)b$, which is the desired relationship corresponding precisely to the first equation when expressions for a and b are substituted and when $m = k-2$.

In addition to the relationships given in the above lemma, yet one more relationship must be established in order that ψ_k vanish at all partition points except r_k. The final relationship from the partition point vanishing condition is given by the following:

LEMMA 2. *Let ψ_k be the piecewise quadratic functions over the interlaced mesh of Lemma* 1 *as illustrated in Fig.* 3. *Then the function maximum $\psi_k(r_k) = \max_r \psi_k(r)$ is a positive quantity that is given by both*

$$\psi_k(r_k) = \tfrac{1}{2}h_{k-1}[\alpha_{k-1}\psi'_k(r_{k-1}) + \psi'_k(w_{k-1})] \tag{5a}$$

and

$$\psi_k(r_k) = -\tfrac{1}{2}h_k[(1-\alpha_k)\,\psi'_k(r_{k+1}) + \psi'_k(w_k)], \tag{5b}$$

for $1 < k < N-1$ and by

$$\psi_1(r_1) = -\tfrac{1}{2}h_1[\alpha_1\psi'_1(r_1) + \psi'_1(w_1) + (1-\alpha_1)\,\psi'_1(r_2)] \tag{5c}$$

and

$$\psi_{N-1}(r_{N-1}) = \tfrac{1}{2}h_{N-2}[\alpha_{N-2}\psi'_{N-1}(r_{N-2}) + \psi'_{N-1}(w_{N-2}) + (1-\alpha_{N-2})\,\psi'_{N-1}(r_{N-1})], \tag{5d}$$

for the respective endpoints.

Proof. Suppose that $1 < k < N-1$. Then since $\psi_k(r_{k-1}) = \psi_k(r_{k+1}) = 0$, an application of the fundamental theorem of calculus implies that the integral of ψ'_k from r_{k-1} to r_{k+1} must vanish. Moreover, since $\psi'_k(r)$ is positive for $r_{k-1} < r < r_k$ and negative for $r_k < r < r_{k+1}$, the maximum of ψ_k is given by

$$\psi_k(r_k) = \int_{r_{k-1}}^{r_k} \psi'_k(x)\,dx = -\int_{r_k}^{r_{k+1}} \psi'_k(x)\,dx. \tag{6}$$

From an observation of Figs. 4b–d, each integral is equal to the sum of a triangular and a trapezoidal area. Upon substitution of each sum, Eqs. (5a) and (5b) result.

Now consider the endpoint function ψ_1 associated with r_1. Since $\psi_1(r_2)$ vanishes, an application of the fundamental theorem of calculus yields the integral representation

$$\psi_1(r_1) = -\int_{r_1}^{r_2} \psi_1'(x)\, dx. \tag{7}$$

Eq. (5c) is then obtained from an evaluation of the integral as the sum of the two trapezoidal areas which are evident upon examination of Fig. 4a. By a similar argument, Eq. (5d) is obtained for the endpoint function ψ_{N-1} associated with r_{N-1} and with the derivative illustrated in Fig. 4e.

Under the constraints derived above, the class of piecewise quadratic functions satisfy the required interpolation conditions but may fail to satisfy any specification for either local or global uniformity in the distribution of coordinate surfaces with constant r. Consequently, further constraints must be considered so that such specifications of uniformity will be possible. These constraints, unlike the previous ones, will result in relationships between distinct piecewise quadratic functions. In the multisurface transformation, the uniformity is along each coordinate curve in the r variable; it is measured by projections onto line segments, the arc length of which can be used as a yardstick to indicate locations in the spanwise direction between bounding surfaces. For uniform conditions to exist, [1, Theorem 1] must be satisfied. In particular, the interpolation functions must satisfy Eq. (2), or equivalently, the derivative of Eq. (2) which is given by

$$\sum_{k=1}^{N-1} \frac{\psi_k'(r)}{\psi_k(r_k)} = 0. \tag{8}$$

Since the multisurface transformation (Eq. (1)) remains unchanged when the interpolation functions are multiplied by real numbers, there is no loss of generality in setting

$$\psi_1(r_1) = \cdots = \psi_k(r_k) = \cdots = \psi_{N-1}(r_{N-1}), \tag{9}$$

which can be obtained by a selection of suitable factors. When Eq. (9) is substituted into Eq. (8), the uniformity condition reduces to the simple form

$$\sum_{k=1}^{N-1} \psi_k'(r) = 0. \tag{10}$$

For the piecewise quadratic representation, the sum in Eq. (10) is a continuous piecewise linear function with junctures between segments only at points of the interlaced mesh, illustrated in Fig. 4. The vanishing condition now reduces to a

requirement that the sum vanish at each point of the interlaced mesh. Due to the local definition of the interpolation functions, the sum contains only three terms on the endpoint intervals $[r_1, r_2)$ and $[r_{N-2}, r_{N-1}]$ and four terms on the interior intervals $[r_k, r_{k+1})$ for $k = 2,..., N-3$. Upon evaluation at the partition points, the uniformity condition becomes

$$\psi_1'(r_1) + \psi_2'(r_1) = 0, \tag{11a}$$

$$\psi_{N-2}'(r_{N-1}) + \psi_{N-1}'(r_{N-1}) = 0, \tag{11b}$$

for endpoints and

$$\psi_{k-1}'(r_k) + \psi_{k+1}'(r_k) = 0, \tag{11c}$$

for $k = 2, 3,..., N-2$. There are only two terms in each of these equations, since the possibly remaining terms each vanished, as can be observed from Fig. 4c. By contrast, the evaluation at the juncture points $(w_1, w_2,..., w_{N-2})$ contains a contribution from each possible term. The uniformity condition here is then given by

$$\psi_1'(w_1) + \psi_2'(w_1) + \psi_3'(w_1) = 0, \tag{12a}$$

$$\psi_{N-3}'(w_{N-2}) + \psi_{N-2}'(w_{N-2}) + \psi_{N-1}'(w_{N-2}) = 0, \tag{12b}$$

for endpoint intervals and

$$\psi_{k-1}'(w_k) + \psi_k'(w_k) + \psi_{k+1}'(w_k) + \psi_{k+2}'(w_k) = 0, \tag{12c}$$

for $k = 2, 3,..., N-3$. By use of Lemmas 1 and 2, the evaluations at the juncture points can each be expressed in terms of partition point evaluations of the interpolation functions and their derivatives. When the resultant expressions are then combined with the unformity condition for partition points (Eq. (11)), the sequence of equalities of Eq. (9) can be retrieved as a check on consistency. The admissibility and application of uniformity can now be summarized in the following form:

THEOREM 3. *Either local or global uniformity in the distribution of constant r coordinate surfaces can be specified with the piecewise quadratic interpolants which satisfy the sequence of equalities in Eq.* (9) *and the derivative conditions in Eqs.* (11) *and* (12). *Uniformity is then specified by a direct application of Eqs.* (5b) *and* (9) *from* [1, *Theorem* 1].

THE EXPLICIT CONSTRUCTION OF THE PIECEWISE QUADRATIC INTERPOLATION FUNCTIONS

With the interpolatory and uniformity constraints just given, suitable piecewise quadratic functions can now be explicitly constructed for the multisurface transformation. To simplify the algebraic expressions, some notation will be introduced. In particular, let the sequence of equalities from Eq. (9) be denoted by

$$A = \psi_k(r_k), \tag{13a}$$

for $k = 1,..., N-1$; let $b_{N-1} = \psi'_{N-1}(r_{N-1})$; and let

$$b_k = \psi'_{k+1}(r_k), \tag{13b}$$

$$c_k = -\psi'_k(w_k), \tag{13c}$$

$$d_{k+1} = \psi'_{k+1}(w_k), \tag{13d}$$

for $k = 1, 2,..., N-2$, where as before the juncture point (w_k) evaluations can be taken from Lemma 2. From Fig. 4, it is clear that each of the notations is a positive number. From Eq. (11) for the uniformity condition at partition points, it is also clear that b_k is associated only with the partition point r_k for each k rather than any specific interpolation function. As a consequence, b_k should be proportional to the curvature at r_k on the coordinate curves in the r variable since it would then appear as a linear multiplier in the second r derivative of the multisurface transformation evaluated at r_k. For further notational simplifications, let

$$I_k^- = (w_{k-1}, r_k], \tag{14a}$$

and

$$I_k^+ = (r_k, w_k], \tag{14b}$$

be the intervals on either side of r_k for $k = 2, 3,..., N-2$. To complete this notation, let $I_1^+ = [r_1, w_1]$ and $I_{N-1}^- = (w_{N-2}, r_{N-1}]$. Since the interpolation functions at and near the boundaries differ slightly from the general form, the construction of the general form shall precede the others throughout the development. With this ordering, the analytic expression for the derivative of the general interpolation function, illustrated in Fig. 4c, is obtained directly from the function values on the interlaced mesh. In terms of the established notation, the result is given by

$$\begin{aligned}
\psi'_k(r) &= -[(1-\alpha_{k-2})\, b_{k-1}/\alpha_{k-2} h_{k-2}](r - r_{k-2}), && \text{on } I_{k-2}^+,\\
&= b_{k-1}[1 - [(2-\alpha_{k-2})/(1-\alpha_{k-2})\, h_{k-2}](r_{k-1} - r)], && \text{on } I_{k-1}^-,\\
&= [(d_k - b_{k-1})/\alpha_{k-1} h_{k-1}](r - r_{k-1}) + b_{k-1}, && \text{on } I_{k-1}^+,\\
&= (d_k/(1-\alpha_k)\, h_{k-1})(r_k - r), && \text{on } I_k^-,\\
&= -(c_k/\alpha_k h_k)(r - r_k), && \text{on } I_k^+,\\
&= [(b_{k+1} - c_k)/(1-\alpha_k)\, h_k](r_{k+1} - r) - b_{k+1}, && \text{on } I_{k+1}^-,\\
&= b_{k+1}[((1+\alpha_{k+1})/\alpha_{k+1} h_{k+1})(r - r_{k+1}) - 1], && \text{on } I_{k+1}^+,\\
&= [\alpha_{k+1} b_{k+1}/(1-\alpha_{k+1})\, h_{k+1}](r_{k+2} - r), && \text{on } I_{k+2}^-,\\
&= 0, && \text{otherwise.}
\end{aligned} \tag{15}$$

Suitably truncated versions of this function are also valid for $k = 2$ and $N - 2$ in correspondence with Figs. 4b and d. For $k = 1$ and $N - 1$, however, in correspondence with Figs. 4a and e, a line segment has been changed. In the case of $k = 1$, the new segment is given by

$$\psi_1'(r) = [(b_1 - c_1)/\alpha_1 h_1](r - r_1) - b_1, \tag{16}$$

on I_1^+. On the remaining intervals, ψ_1' is given by the general form above. Similarly, ψ_{N-1}' is given by

$$\psi_{N-1}'(r) = [(d_{N-1} - b_{N-1})/(1 - \alpha_{N-2})\, h_{N-2}](r_{N-1} - r) + b_{N-1}, \tag{17}$$

on I_{N-1}^- and assumes the general form elsewhere. With the notation of Eq. (13) and the results of Lemma 2, the derivative evaluations at w_k are given by

$$c_1 = (2A/h_1) - \alpha_1 b_1 - (1 - \alpha_1)\, b_2, \tag{18a}$$

$$d_{N-1} = (2A/h_{N-2}) - \alpha_{N-2} b_{N-2} - (1 - \alpha_{N-2})\, b_{N-1}, \tag{18b}$$

and

$$c_k = (2A/h_k) - (1 - \alpha_k)\, b_{k+1}, \tag{18c}$$

$$d_k = (2A/h_{k-1}) - \alpha_{k-1} b_{k-1}, \tag{18d}$$

for $k = 2, 3, \ldots, N - 2$.

To obtain the desired piecewise quadratic interpolation functions, each of the continuous piecewise linear derivative functions must be integrated. For k between 3 and $N - 3$, the result is given by

$$\begin{aligned}
\psi_k(r) &= -[(1 - \alpha_{k-2})\, b_{k-1}/2\alpha_{k-2} h_{k-2}](r - r_{k-2})^2, && \text{on } I_{k-2}^+,\\
&= [(2 - \alpha_{k-2}) b_{k-1}/2(1 + \alpha_{k-2}) h_{k-2}](r_{k-1} - r)^2 - b_{k-1}(r_{k-1} - r), && \text{on } I_{k-1}^-,\\
&= [(d_k - b_{k-1})/2\alpha_{k-1} h_{k-1}](r - r_{k-1})^2 + b_{k-1}(r - r_{k-1}), && \text{on } I_{k-1}^+,\\
&= (-d_k/2(1 - \alpha_{k-1})\, h_{k-1})(r_k - r)^2 + A, && \text{on } I_k^-,\\
&= (-c_k/2\alpha_k h_k)(r - r_k)^2 + A, && \text{on } I_k^+,\\
&= [(c_k - b_{k+1})/2(1 - \alpha_k)\, h_k](r_{k+1} - r)^2 + b_{k+1}(r_{k+1} - r), && \text{on } I_{k+1}^-,\\
&= [(1 + \alpha_{k+1})\, b_{k+1}/2\alpha_{k+1} h_{k+1}](r - r_{k+1})^2 - b_{k+1}(r - r_{k+1}), && \text{on } I_{k+1}^+,\\
&= -[\alpha_{k+1} b_{k+1}/2(1 - \alpha_{k+1})\, h_{k+1}](r_{k+2} - r)^2, && \text{on } I_{k+2}^-,\\
&= 0, && \text{otherwise,}
\end{aligned} \tag{19}$$

which is continuous up through first derivatives and is illustrated in Fig. 3c. For $k = 2$, $N - 2$, the interpolation functions are just suitably truncated versions of the general function and are illustrated in Figs. 3b and d.

In the special case when $k = 1$, a direct integration yields

$$\psi_1(r) = [(b_1 - c_1)/2\alpha_1 h_1](r - r_1)^2 - b_1(r - r_1) + A \tag{20}$$

on I_1^+, where the constant of integration was obtained from the condition $\psi_1(r_1) = A$. On the remaining intervals, ψ_1 coincides with the general form with $k = 1$ and is easily seen to be continuous up through first derivatives at $r_1 + \alpha_1 h_1$ upon substitution for c_1 from Eq. (18a). Similarly, for $k = N - 1$, an integration yields

$$\psi_{N-1}(r) = [(b_{N-1} - d_{N-1})/2(1 - \alpha_{N-1})h_{N-1}](r - r_{N-1})^2 + b_{N-1}(r - r_{N-1}) + A \tag{21}$$

on I_{N-1} which is joined to the general form with $k = N - 1$ to obtain ψ_{N-1} as a function with continuity up through first derivatives. The interpolation functions ψ_1 and ψ_{N-1} are illustrated in Figs. 3a and e, respectively.

To obtain the multisurface transformation (Eq. (1a)), the integrals $G_k(r)$ in Eq. (1b) must be computed for $k = 1, 2, \ldots, N - 1$. The computations involve a direct substitution and a subsequent integration which requires some algebra in the determination of appropriate constants of integration for each quadratic segment. In the general case when $3 \leqslant k \leqslant N - 3$, the result is given by

$$\begin{aligned}
G_k(r) &= 0, && \text{for } r \leqslant r_{k-2},\\
&= -[(1 - \alpha_{k-2})\, b_{k-1}/6\alpha_{k-2} h_{k-2}](r - r_{k-2})^3, && \text{on } I_{k-2}^+,\\
&= -\frac{(2 - \alpha_{k-2})\, b_{k-1}}{6(1 - \alpha_{k-2})\, h_{k-2}}(r_{k-1} - r)^3 + \frac{b_{k-1}}{2}(r_{k-1} - r)^2 + G_k(r_{k-1}) && \text{on } I_{k-1}^-,\\
&= \frac{d_k - b_{k-1}}{6\alpha_{k-1} h_{k-1}}(r - r_{k-1})^3 + \frac{b_{k-1}}{2}(r - r_{k-1})^2 + G_k(r_{k-1}) && \text{on } I_{k-1}^+,\\
&= (d_k/6(1 - \alpha_{k-1})\, h_{k-1})(r_k - r)^3 - A(r_k - r) + G_k(r_k) && \text{on } I_k^-,\\
&= -(c_k/6\alpha_k h_k)(r - r_k)^3 + A(r - r_k) + G_k(r_k) && \text{on } I_k^+,\\
&= \frac{b_{k+1} - c_k}{6(1 - \alpha_k)\, h_k}(r_{k+1} - r)^3 - \frac{b_{k+1}}{2}(r_{k+1} - r)^2 + G_k(r_{k+1}) && \text{on } I_{k+1}^-,\\
&= \frac{(1 + \alpha_{k+1})\, b_{k+1}}{6\alpha_{k+1} h_{k+1}}(r - r_{k+1})^3 - \frac{b_{k+1}}{2}(r - r_{k+1})^2 + G_k(r_{k+1}) && \text{on } I_{k+1}^+,\\
&= (\alpha_{k+1} b_{k+1}/6(1 - \alpha_{k+1})\, h_{k+1})(r_{k+2} - r)^3 + G_k(r_{k+2}) && \text{on } I_{k+2}^-,\\
&= G_k(r_{k+2}) && \text{for } r \geqslant r_{k+2},
\end{aligned} \tag{22}$$

where

$$G_k(r_{k-1}) = -\tfrac{1}{6}(1-\alpha_{k-2})\, b_{k-1} h_{k-2}^2, \tag{23a}$$

$$G_k(r_k) - G_k(r_{k-1}) = \tfrac{1}{3}A(2-\alpha_{k-1})\, h_{k-1} + \tfrac{1}{6}\alpha_{k-1} b_{k-1} h_{k-1}^2, \tag{23b}$$

$$G_k(r_{k+1}) - G_k(r_k) = \tfrac{1}{3}A(1+\alpha_k)\, h_k + \tfrac{1}{6}(1-\alpha_k)\, b_{k+1} h_k^2, \tag{23c}$$

and

$$G_k(r_{k+2}) - G_k(r_{k+1}) = -\tfrac{1}{6}\alpha_{k+1} b_{k+1} h_{k+1}^2. \tag{23d}$$

When $k=2$, the general formulation above is modified by removing the first three entries and setting $G_2(r_1)=0$. Similarly, for $k=N-2$, the last three entries are removed and the last increment (Eq. (23d)) for integration constants in Eq. (23) is deleted. When $k=1$, a direct integration of Eq. (20) yields

$$G_1(r) = [(b_1 - c_1)/6\alpha_1 h_1](r-r_1)^3 - \tfrac{1}{2}b_1(r-r_1)^2 + A(r-r_1), \tag{24}$$

on I_1^+, where the constant of 0 was chosen to satisfy $G_1(r_1)=0$. On the remaining intervals, it coincides with the last four entires of the general form, except with different constants of integration. From a direct integration,

$$G_1(r_2) - G_1(r_1) = \tfrac{1}{3}A(1+\alpha_1)\, h_1 + \tfrac{1}{6}(1-\alpha_1)\, b_2 h_1^2 - \tfrac{1}{6}\alpha_1 b_1 h_1^2, \tag{25a}$$

and from the general form

$$G_1(r_3) - G_1(r_2) = -\tfrac{1}{6}\alpha_2 b_2 h_2^2, \tag{25b}$$

which together yield the necessary constants of integration. On the other side when $k=N-1$, the integral coincides with the first four entries of the general form including the constant of integration

$$G_{N-1}(r_{N-2}) = -\tfrac{1}{6}(1-\alpha_{N-3})\, b_{N-2} h_{N-3}^2. \tag{26}$$

By integration of Eq. (21), the last segment becomes

$$G_{N-1}(r) = \frac{d_{N-1} - b_{N-1}}{6(1-\alpha_{N-2})\, h_{N-2}} (r_{N-1} - r)^3 + \tfrac{1}{2}b_{N-1}(r_{N-1} - r)^2 - A(r_{N-1} - r) + G_{N-1}(r_{N-1}), \tag{27}$$

over I_{N-1}^-. The constant of integration, determined by continuity, is given by

$$G_{N-1}(r_{N-1}) - G_{N-1}(r_{N-2}) = \tfrac{1}{3}A(2-\alpha_{N-2})\, h_{N-2} + \tfrac{1}{6}\alpha_{N-2} b_{N-2} h_{N-2}^2 - \tfrac{1}{6}(1-\alpha_{N-2})\, b_{N-1} h_{N-2}^2, \tag{28}$$

which completes the computation of the integrals of the interpolation functions. An illustration of these results is given in Fig. 6, which has a format in correspondence

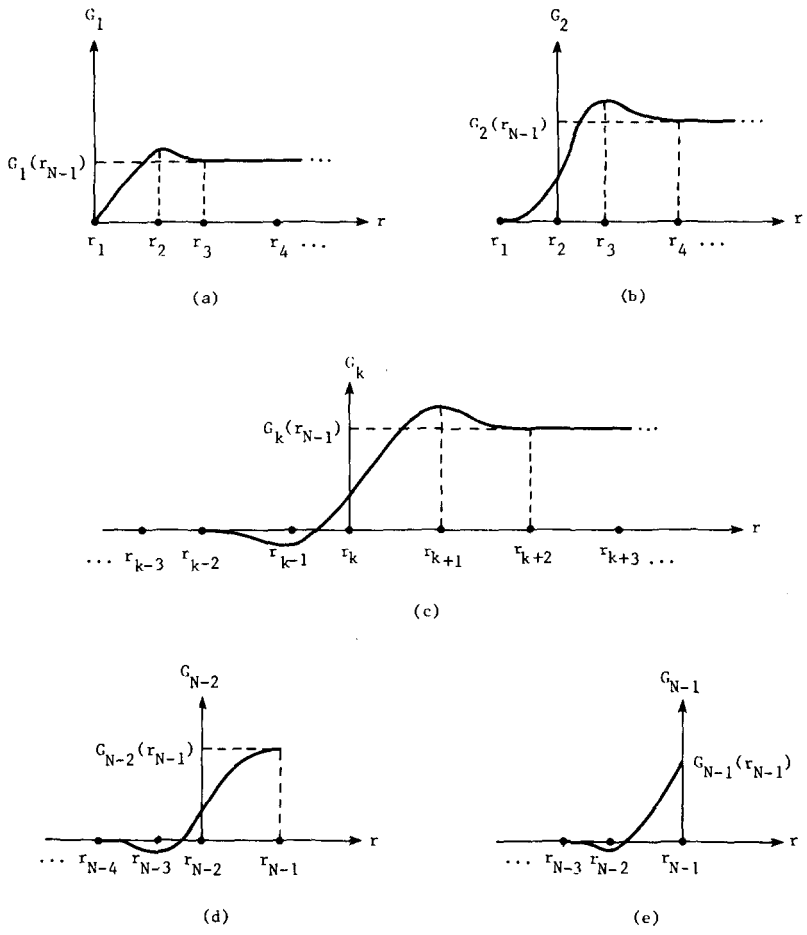

FIG. 6. Integrals of the piecewise quadratic interpolation functions.

with the previous displays given in Figs. 3 and 4, respectively. The general form in Fig. 6c is seen to leave 0 at r_{k-2}, decrease to a local minimum at r_{k-1}, increase to a local maximum at r_{k+1}, and decrease to a saturation value of $G_k(r_{N-1})$ at r_{k+2}. In the other parts, truncated versions of the general form are vertically lifted or dropped so that each is smoothly connected to the r axis.

PARTITION POINT EVALUATIONS

In the case of C^0 interpolants, the partition point evaluations were especially valuable since a simple geometric interpretation was available, namely, that the coor-

dinate curves in the r variable passed through or touched line segments determined by the basic constructive surfaces in the multisurface transformation (Eq. (1)). When the evaluations were combined with curvature properties, there was a corresponding approximation property where convexity and monotonicity were preserved from the data given by points on the constructive surfaces with a fixed t. Moreover, when the simple geometric interpretation of the evaluations was used to interchange constructive surface data with the evaluations, a comonotone and coconvex interpolation scheme was obtained. In a similar vein, the partition point evaluations will be pursued for the case with C^1 interpolations and with a goal which is only to obtain a simple geometric interpretation.

When the integrals (Eqs. (22)–(28)) of the local C^1 interpolants are inserted into the multisurface transformation (Eq. (1)), the collapsed form

$$\mathbf{P}(r, \mathbf{t}) = \mathbf{P}_{m-1}(\mathbf{t}) + \sum_{k=m-1}^{m+2} \frac{G_k(r)}{G_k(r_{N-1})} [\mathbf{P}_{k+1}(\mathbf{t}) - \mathbf{P}_k(\mathbf{t})] \tag{29}$$

is obtained for $r_m \leqslant r < r_{m+1}$. In parallel with the earlier C^0 case, the surface $\mathbf{P}_1(\mathbf{t})$ and the first $m-2$ terms in the sum telescopically collapsed into $\mathbf{P}_{m-1}(\mathbf{t})$, while the last $(N-1)-(m+2)$ terms vanished for the given values of r. Since $G_{m+2}(r_m) = 0$, the evaluation of Eq. (29) at the partition point $r = r_m$ contains only the first three terms in the sum. Upon rearrangement, the result becomes

$$\mathbf{P}(r_m, \mathbf{t}) = \mathbf{W}_m + \left[\frac{G_{m-1}(r_m)}{G_{m-1}(r_{N-1})} - 1 \right] [\mathbf{P}_m - \mathbf{P}_{m-1}] - \frac{G_{m+1}(r_m)}{G_{m+1}(r_{N-1})} [\mathbf{P}_{m+1} - \mathbf{P}_{m+2}], \tag{30a}$$

where

$$\mathbf{W}_m = [1 - (G_m(r_m)/G_m(r_{N-1}))] \mathbf{P}_m + (G_m(r_m)/G_m(r_{N-1})) \mathbf{P}_{m+1}, \tag{30b}$$

and for simplicity of notation, the $\mathbf{t}$ dependence is not explicitly displayed. Since the coefficients in the expression for $\mathbf{W}_m$ are bounded between 0 and 1 and sum to unity, the point $\mathbf{W}_m$ lies on the line segment between $\mathbf{P}_m$ and $\mathbf{P}_{m+1}$ for each fixed value of $\mathbf{t}$. From Eqs. (22)–(28) or by direct observation of Fig. 6, $G_{m-1}(r_m)/G_{m-1}(r_{N-1})$ is seen to be slightly greater than unity and $G_{m+1}(r_m)/G_{m+1}(r_{N-1})$ is seen to be a small negative number. As a consequence, the partition point evaluation in Eq. (30a) is geometrically computed by locating the point $\mathbf{W}_m$ on the above line segment and adding to it two small vector quantities respectively in the positive $\mathbf{P}_m - \mathbf{P}_{m-1}$ and $\mathbf{P}_{m+1} - \mathbf{P}_{m+2}$ directions. An illustration of this geometric interpretation is given in Fig. 7. The principal difference from the earlier C^0 case lies in the addition of the two small vector quantities.

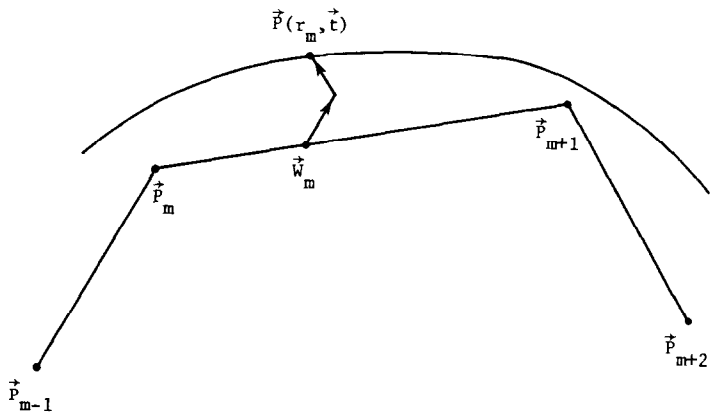

FIG. 7. Geometric construction of a partition point evaluation.

LOCAL C^m INTERPOLATION FUNCTIONS

Local interpolation functions for the multisurface transformation (Eq. (1)) have been constructed as functions with C^0 and C^1 smoothness, respectively. In correspondence with an increase in required smoothness, the size of the local region of nontrivial values had to be increased for each interpolation function. In particular, when smoothness was increased from C^0 to C^1, a local region determined by three consecutive partition points had to be increased by the addition of a partition point on each side. That is, three consecutive points determining an interval had to be replaced by five. With further demands for smoothness, it is reasonable to expect the above pattern to continue, with the extension of the local region by a partition point on each side for every added level of differentiability. In Fig. 8, the sequence of general interpolation functions are graphically displayed in correspondence with a noted level of smoothness. Basic requirements for canonical interpolation ($\psi_k(r_j) = \psi_k(r_k)\,\delta_{kj}$) and for simplicity are evident from the illustrations. By contrast, uniformity requirements are more subtle and cannot be readily illustrated in the graphs of function values. To see this, recall that in the C^1 case, uniformity in the distribution of constant r surfaces was clear only by examination of second derivatives. In continuation, the sequence of local interpolation functions can be extended to infinity for C^∞ smoothness. To see how the extension can be accomplished, consider the case where the variable r is uniformly partitioned by setting $r_j = j/2\Omega$ for all integers j and for a real number Ω. With the uniform partition, the functions

$$\psi_k(r) = \sin \pi(2\Omega r - k)/\pi(2\Omega r - k) \tag{31}$$

clearly satisfy a canonical property $\psi_k(r_j) = \delta_{kj}$ and can be considered as local inter-

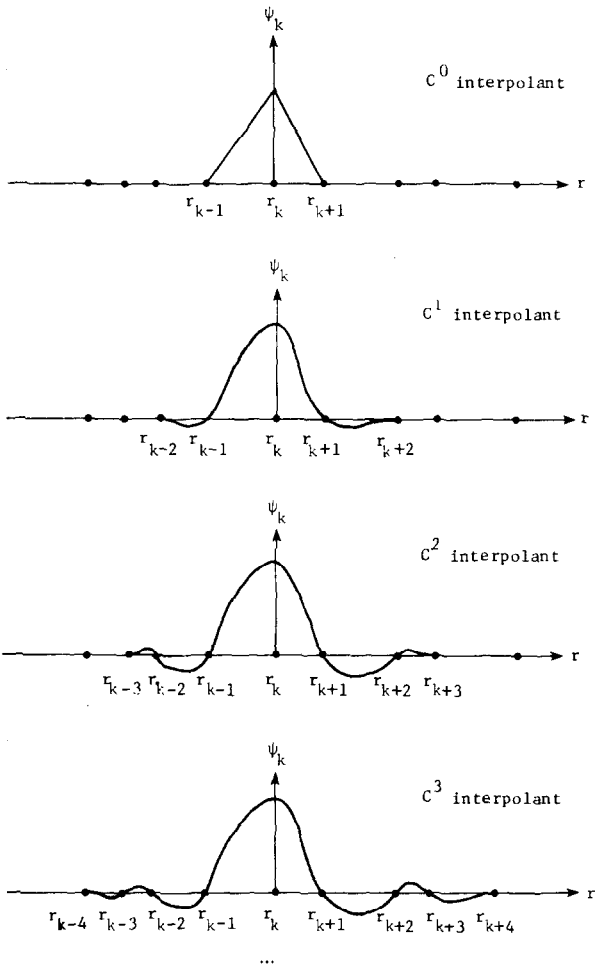

FIG. 8. Sequence of local interpolation functions in the order of increasing smoothness.

polations since the influence of each is locally concentrated at its center. The graphical form of Eq. (31) is easily seen to be a direct continuation of the truncated forms illustrated in Fig. 8, when a uniform partition is assumed. The interpolated vector field, as an extension of the earlier case, is then given by

$$\mathbf{V}(r, \mathbf{t}) = \sum_{k=-\infty}^{\infty} \psi_k(r)\, \mathbf{V}_k(\mathbf{t}), \tag{32}$$

where each $\mathbf{V}_k(\mathbf{t})$ is given by [1, Eq. (3)]. The statement in Eq. (32) is just a vector field version of the sampling theorem which is valid only when the vector field

components are band-limited functions, each with a bandwidth less than Ω. That is, the bilateral Fourier transform must be bounded in absolute value by Ω for each vector component. For more details on the sampling theorem for functions, an excellent presentation is given by Hamming [3]. When Eq. (32) can be integrated term by term, the multisurface transformation becomes

$$\mathbf{P}(r, \mathbf{t}) = \sum_{k=-\infty}^{\infty} \frac{G_k(r)}{G_k(\infty)} [\mathbf{P}_{k+1}(\mathbf{t}) - \mathbf{P}_k(\mathbf{t})], \tag{33a}$$

where

$$G_k(r) = \int_{-\infty}^{r} \psi_k(x)\, dx. \tag{33b}$$

With the interpolation functions of Eq. (31), it is clear that all $G_k(\infty)$ are equal. In addition, the infinite number of constructive surfaces $\mathbf{P}_k(\mathbf{t})$ can be chosen for coordinate generation on either bounded or unbounded regions. Moreover, the infinite case given in Eq. (33) is applicable to all interpolants studied herein, such as those illustrated in Fig. 8 or of the type in Eq. (31).

Conclusion

Coordinate generation techniques with precise local controls have been derived and analyzed for continuity requirements up to both first and second derivatives and have been projected to higher level continuity requirements from the established pattern. The desired precision of the local controls was obtained when a family of coordinate surfaces could be uniformly distributed without a consequent creation of flat spots on the coordinate curves transverse to the family. Relative to the uniform distribution, the family could be redistributed from an a priori distribution function or from a solution adaptive approach, both without distortion from the underlying transformation which may be independently chosen to fit a nontrivial geometry and topology. To explicitly demonstrate the basic power that comes with the precise local controls, examples have been given in Eiseman [1] for systems about airfoils and in Eiseman [4] for a smooth transition from a Cartesian structure to a polar one. In addition, further examples will also be presented when the associated automatic mesh generation algorithm is presented. The algorithm was developed under NASA Lewis Research Center Contract No. NAS3-22117 and was based upon the theory developed herein.

References

1. P. R. Eiseman, *J. Comput. Phys.* **47** (1982), 331.
2. D. Laugwitz, "Differential and Riemannian Geometry," Academic Press, New York, 1965.

3. R. W. HAMMING, "Numerical Methods for Scientists and Engineers," 2nd ed., McGraw–Hill, New York, 1973.
4. P. R. EISEMAN, *in* "Proceedings, Seventh International Conference on Numerical Methods in Fluid Dynamics, June 1980," Lecture Notes in Physics, No. 141, pp. 176–181, Springer-Verlag, Berlin, 1981.